

# Wind Study on Isolated High Rise Building: A Computational Fluid Dynamic Approach

T Ashrith <sup>1</sup>, R. Sreenu <sup>2</sup>

1. Student, masters of structural engineering, civil engineering department, Anurag University, Hyderabad.

2. Assistant professor, civil engineering department, Anurag University, Hyderabad.

## Abstract

Wind analysis is a critical aspect of architectural design, ensuring the structural integrity and safety of buildings in diverse environmental conditions. In this study, we investigate the wind behaviour around a unique shaped building from five different angles, each with a 30-degree increment, utilizing the powerful computational fluid dynamics tool ANSYS. Our analysis focuses on understanding the pressure coefficients, and the resulting flow patterns. The results of this comprehensive wind analysis, conducted with ANSYS, reveal several key findings. First, the pressure coefficients vary significantly, indicating regions of high and low pressure on the building's facade. Furthermore, the flow patterns around the building show complicate interactions, suggesting that the formation of vortices and areas of low wind pressure can be challenging to predict. This complexity underscores the importance of a multi-angle approach to wind analysis, as well as the need for advanced simulation and modeling techniques, as embody by ANSYS, to accurately assess wind effects on such unconventional architectural designs. In conclusion, this study, performed using ANSYS software, provides valuable insights into the wind behavior around a unique shaped building, emphasizing the importance of considering multiple angles in the analysis to ensure a holistic understanding of wind-related challenges and opportunities in architectural design.

**Key Words** -ANSYS software, computational fluid dynamics, pressure coefficients and flow patterns.

## 1. Introduction:

In the current global landscape, the skyline of urban environments is dominated by a surge in the construction of unconventional and symmetrical high-rise buildings. This architectural trend, driven by both aesthetics and functional considerations, underscores the need for a meticulous examination of their response to wind forces. The escalating heights and distinctive shapes of these structures demand a tailored approach to wind analysis to comprehend the complex interactions between the built environment and natural elements.

The imperative for wind analysis is further accentuated by the potential risks associated with high winds on skyscrapers. Unchecked wind forces can induce structural vibrations, compromising the overall stability and safety of the building. Computational Fluid Dynamics (CFD) simulations, particularly those conducted using ANSYS, offer a sophisticated means to model and predict wind behavior around these intricate structures. This analytical approach aids in identifying potential pressure points, turbulent zones, and dynamic forces that may affect the building's performance.

Furthermore, the economic implications of inadequate wind analysis cannot be overstated. Failures in predicting and mitigating wind-induced effects may result in costly retrofits, increased maintenance expenses, and even potential legal liabilities. The utilization of advanced tools like CFD in conjunction with ANSYS not only enhances the accuracy of predictions but also facilitates a more cost-effective and sustainable approach to building design and operation.

In a study conducted by Biswarup Bhattacharyya and colleagues in 2014, experimentation focused on the pressure distribution on different faces of 'E' plan-shaped tall buildings under wind excitation. The research utilized wind angles ranging from  $0^\circ$  to  $180^\circ$  at  $30^\circ$  intervals. Experimental investigations took place in an open-circuit boundary layer wind tunnel, while analytical analysis employed the k-e turbulence model and Computational Fluid Dynamics (CFD) technique using the ANSYS CFX software. Mean pressure coefficients for all faces were calculated for various wind angles, and pressure contours were presented for a  $0^\circ$  wind angle.

Another study by Rajdip Paul and team in 2016 delved into the behavior of surfaces of a 'Z' plan-shaped tall building when exposed to different wind directions. Utilizing the ANSYS CFD package with a length scale of one-hundredth of a mile, the research examined wind incidence angles from  $0^\circ$  to  $150^\circ$  at  $30^\circ$  increments. Force coefficients in both along and across wind directions, along with external surface pressure coefficients on different faces of the building, were determined and listed. Flow separation features, vortices, and wind pressure fluctuations on various surfaces were vividly illustrated through contour plots. The study also presented the deviation of external pressure coefficients with building height and around the building perimeter for different wind angles of attack.

In 2017, Fubin Chen explored the wind-induced torques acting on L-shaped tall buildings. The study involved eight L-shaped rigid models with varying geometric dimensions in a boundary wind tunnel. Investigation of wind-induced torques included RMS force coefficients, power spectral densities, and vertical correlation functions. The research proposed empirical methods for predicting wind-induced torques on L-shaped tall buildings based on wind tunnel test findings, highlighting the significance of side ratio and terrain category as crucial variables. The ultimate aim was to develop a simple and effective method for calculating wind-induced torque on L-shaped tall buildings.

In 2016, Sujit Kumar Dalui utilized the computational fluid dynamics module to examine the pressure variations on the faces of an octagonal plan-shaped tall building resulting from the interference of three square plan-shaped tall structures of equal height. The study investigated different scenarios involving the placement of square plan-shaped buildings in isolation and compared them with the octagonal plan-shaped building. In some instances, abnormal pressure distributions were observed. The presence of interfering buildings led to shielding and channeling effects on the octagonal plan-shaped building, making the pressure distribution on its faces unpredictable under interfering conditions. The regularity of the faces' behavior increased as the distance between the main octagonal structure and the third square interfering building grew.

## 2. Numerical Analysis:

### 2.1 Geometry modelling

This building model, meticulously modelled in ANSYS software, exhibits a length and breadth of precisely 120 mm each. A distinguishing feature of the structure is the incorporation of two curves, each possessing a 30 mm radius of curvature. These curves elegantly define the inner contours of the horse-shoe shape, contributing to the

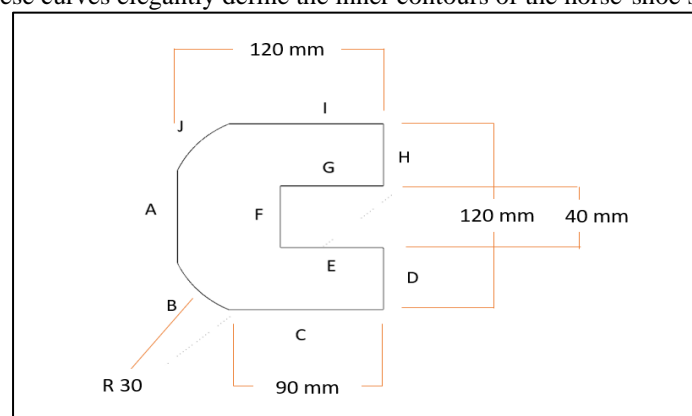


Figure 1: dimensions of the building

architectural intricacy of the design. The spacing between the limbs of the horse-shoe shape is set at 40 mm, further complementing the overall geometry. Additionally, the model has a height of 70 mm, providing a comprehensive dimensional description for accurate simulations in ANSYS. This detailed geometric specification ensures a thorough analysis of the structural and fluid dynamics aspects, enabling precise insights into the behavior of the building under varying conditions.

## 2.2 Meshing

The mesh employed, i.e., the size and shape of the grid, influences the quality of the simulation results. Subsequently, the choice of mesh type comes into focus. For structural analysis, especially for a high-rise building with numerous components, structured and unstructured meshing may be used, but the unstructured grids made up of pyramidal and tetrahedral cells have been avoided in a high-quality body-fitted grid because they can cause

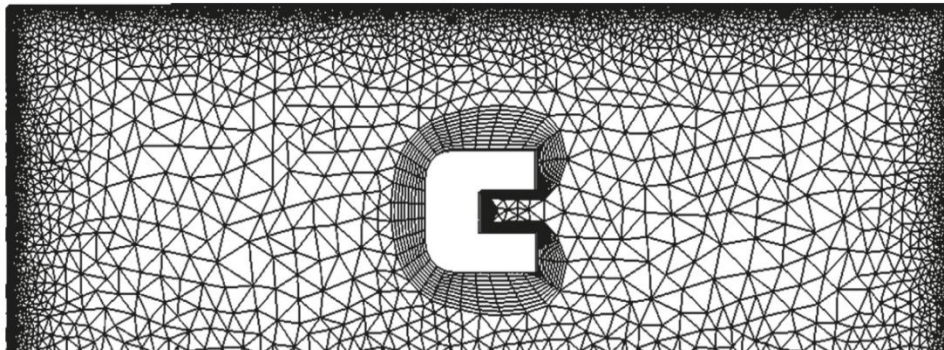


Figure 2: meshing around the building

problems with convergence when employing high-order discretization techniques, lowering computing accuracy. Extreme cell distortion (e.g., angles  $> 90^\circ$  for triangles) are avoided, especially in locations with strong flow gradients. Parallel/perpendicular cells, such as quadrilateral, hexahedral, or prism/wedge cells, are preferred near the walls.

## 2.3 Domain

The dimensions of the computational domain, as illustrated in Figures 3, align with the parameters outlined in Franke et al.'s work [20]. In this configuration, the upstream side is specifically designated as 5 times the height of the building ( $5H$ ) from the building's frontal surface, and the downstream side spans a distance of 15 times the building height ( $15H$ ) from the same reference point.

Moreover, two lateral clearances are assigned, each positioned at a distance of 5 times the building height ( $5H$ ) from the building's frontal surface. Additionally, the upper clearance is defined at 5 times the building height ( $5H$ ) above the building's upper surface. The considerable expansion of the computational domain serves a twofold

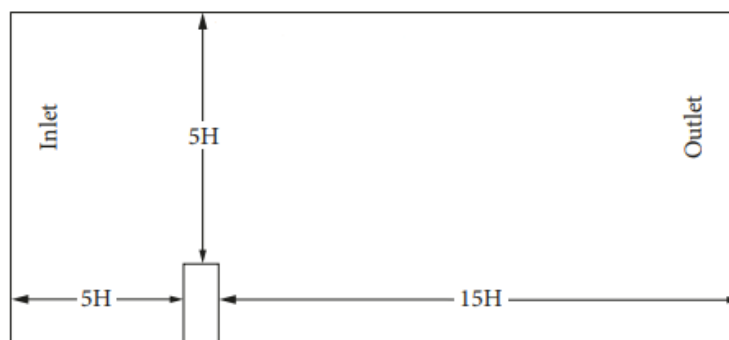


Figure 3: dimensions of the domain

objective: it promotes the formation of vortices on the sheltered side of the building and efficiently hinders wind backflow.

### 2.4 Simulation details

To successfully conduct numerical modeling and simulation, it is crucial to consider multiple boundary conditions, specifically those governing flow parameters at the inlet, outlet wall, and surfaces. At the inlet, the flow velocity is set at 12.9 m/s. It is important to highlight that the flow velocity at the inlet is oriented in the positive X-direction.

Data considered in numerical analysis:		
a	Types of fluid: air	Air
b	Density of air:	1.226 Kg/m <sup>3</sup>
c	Viscosity of air:	$1.7899 \times 10^{-5}$ kg s/m
d	Turbulence model:	k – Epsilon model
e	Velocity of air:	12.9 m/s
f	Solver:	Pressure-based.

**Table: data considered for numerical analysis**

## 3 Results And Discussions:

### 3.1 Wind flow patterns

The pressure distribution on the building is intricately linked to the dynamic wind flow patterns that envelop it. These wind flow patterns give rise to various phenomena, including vortex generation and different flow mechanisms such as separation of flow, upwind and downwind effects. To gain a deeper and more accurate understanding of these mechanisms, a detailed study of wind flow patterns around the horseshoe-shaped building has been conducted. This investigation encompasses wind incidence angles ranging from 0° to 180°, with increments of 30°. The Computational Fluid Dynamics (CFD) technique has been employed to analyze these wind flow patterns

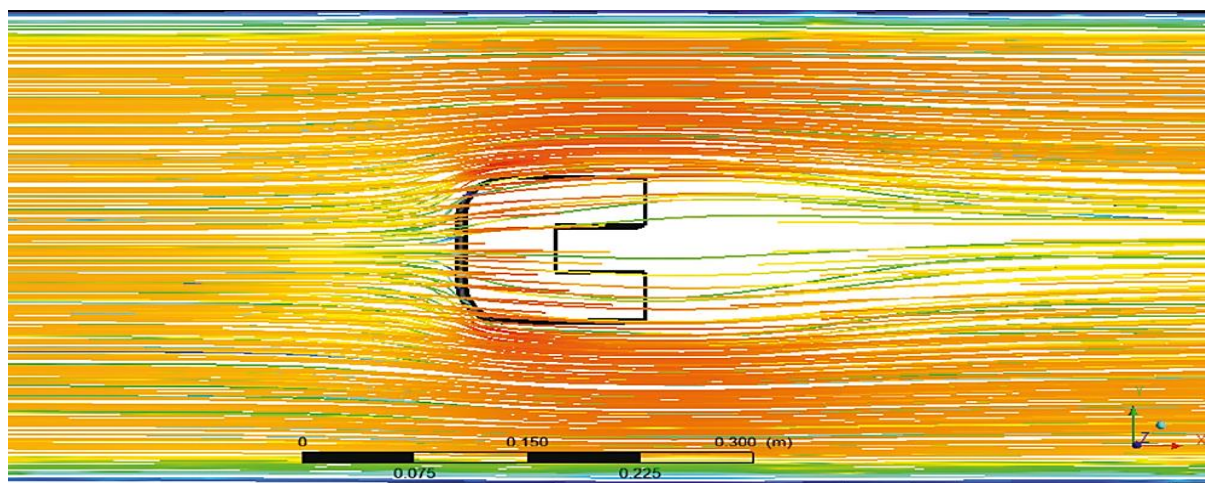


**Figure 4: wind load acting at 0°**

pressure coefficients

The pressure coefficient, often denoted as  $C_p$ , represents the normalized difference between the local pressure at a specific point on the building surface and the free-stream atmospheric pressure. In a building with varying angles, these coefficients are influenced by factors such as geometry, wind direction, and wind speed.

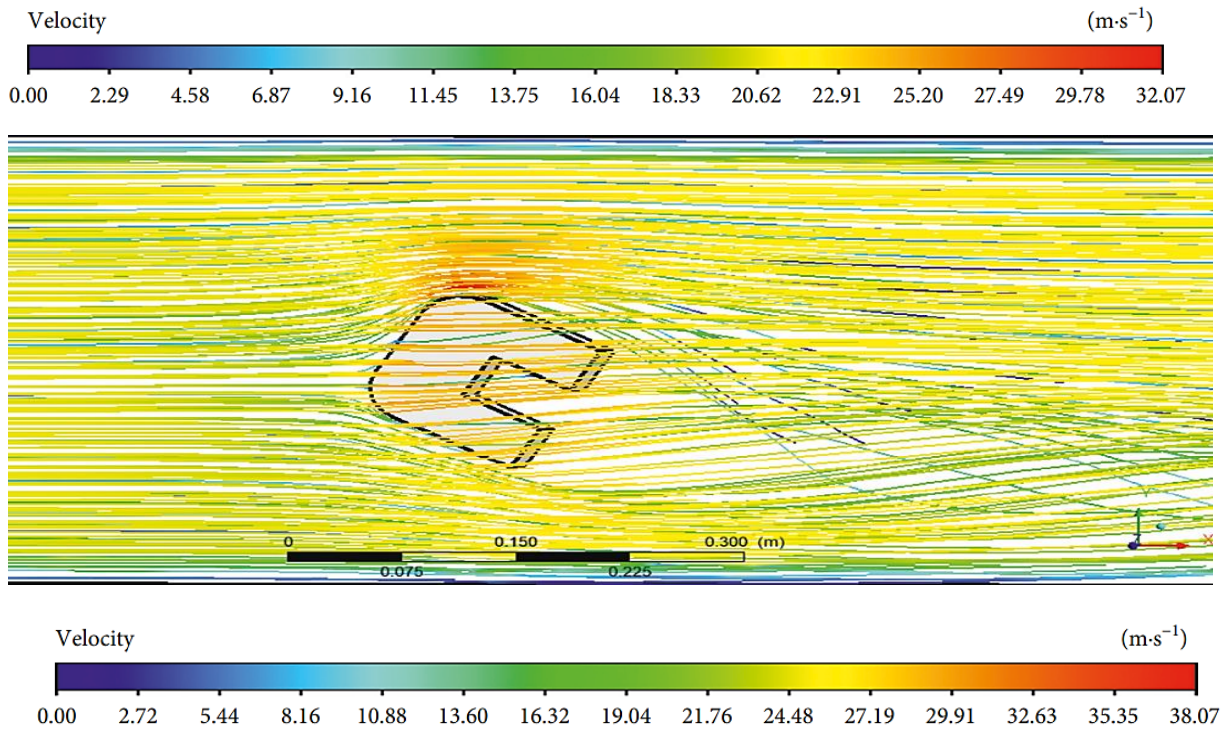


Figure 5: wind load acting at 30°

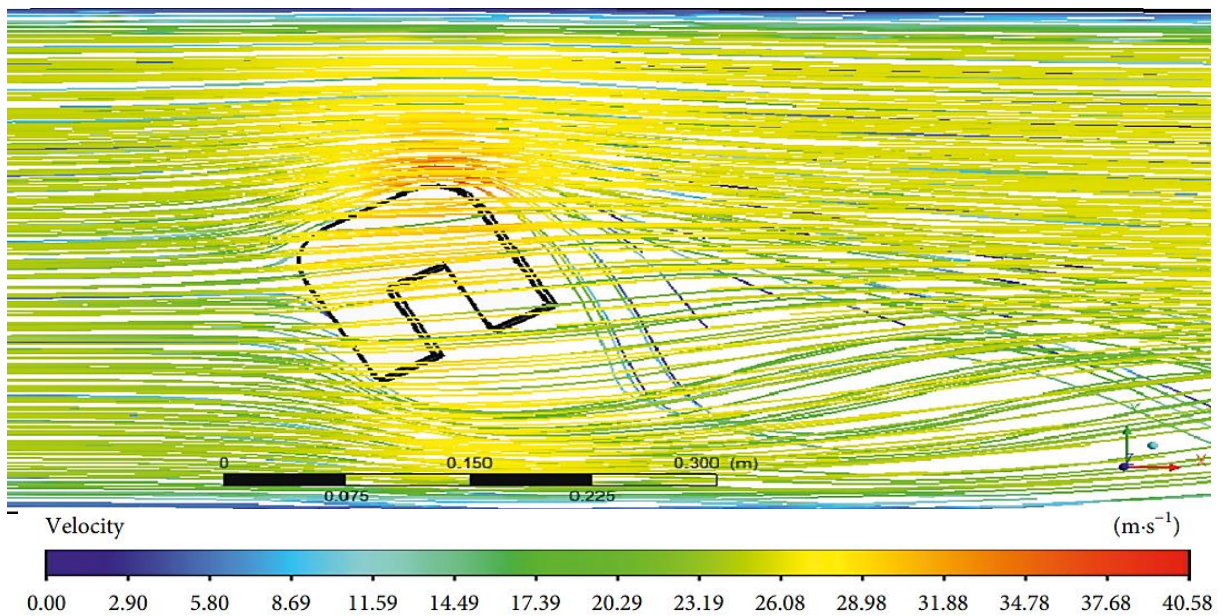


Figure 6: wind load acting at 60°

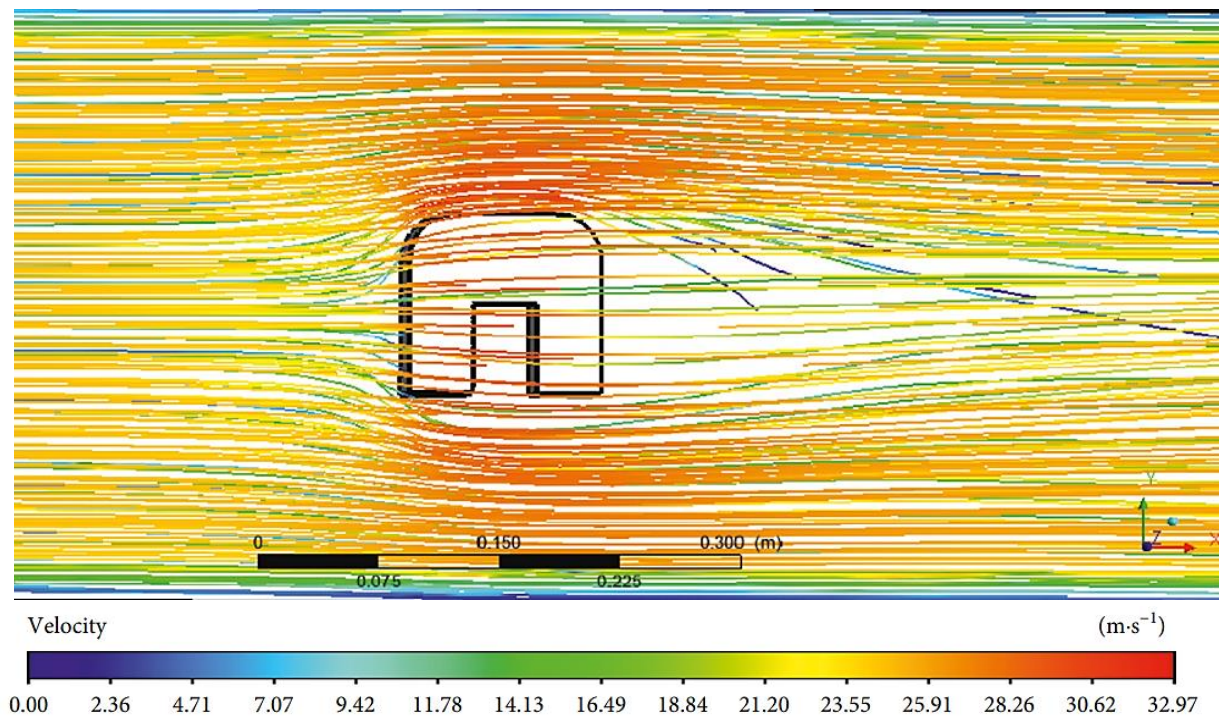


Figure 7: wind load acting at 90<sup>0</sup>

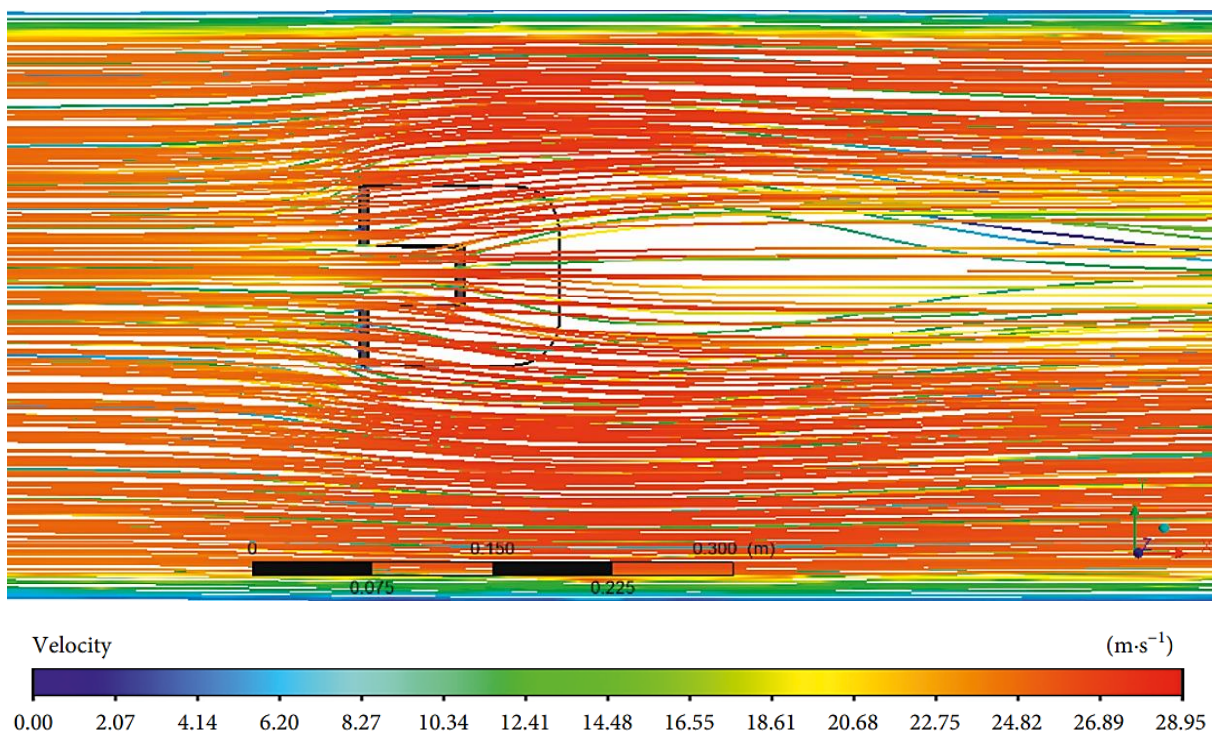
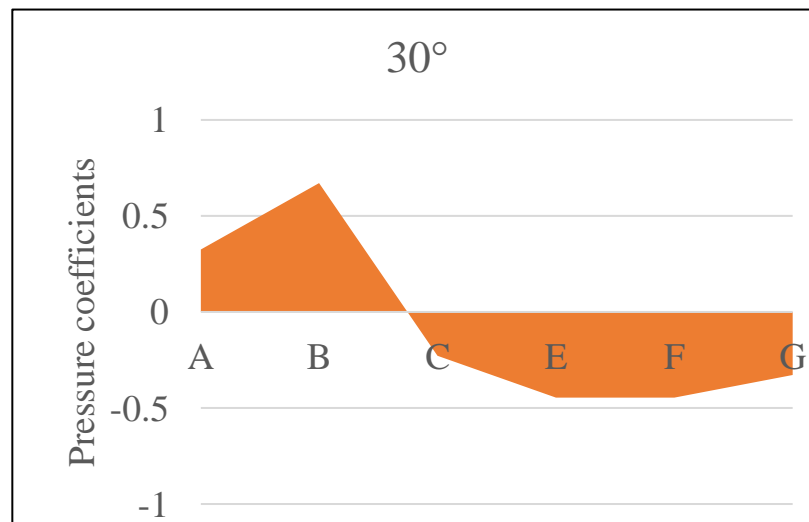


Figure 8: wind load acting at 180<sup>0</sup>

### 3.2 Pressure coefficients

The pressure coefficient, often denoted as  $C_p$ , represents the normalized difference between the local pressure at a specific point on the building surface and the free-stream atmospheric pressure. In a building with varying angles, these coefficients are influenced by factors such as geometry, wind direction, and wind speed.

When the wind exerts its force at a 0-degree angle to the featured building, the specific surface facing the wind,



**Figure 9: variation in pressure coefficients at 0°**

known as face A, undergoes a positive pressure. This means that the air pressure on face A is higher than the ambient atmospheric pressure. Consequently, the coefficients associated with face A also reflect this positive pressure.

On the other hand, faces BCEF and G, representing other surfaces of the building, experience negative pressure coefficients. Negative pressure coefficients indicate that the air pressure on these surfaces is lower than the ambient atmospheric pressure.

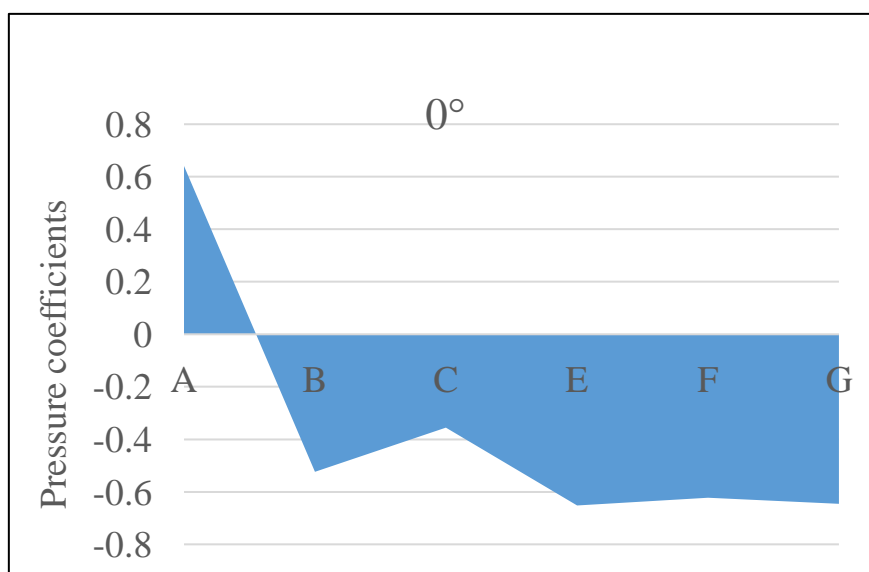


**Figure 10: variation in pressure coefficients at 30°**

When the wind load applies at a 30-degree angle to the highlighted building, the primary surfaces, specifically face A and face B, will encounter positive pressure. Consequently, their corresponding coefficients will also show positive values. Conversely, other surfaces such as CEF and G will experience negative pressure coefficients. At the 30-degree angle, face A, being in closer proximity to face B, undergoes a slightly reduced positive pressure compared to faces CEF and G. The proximity to face B influences the strength of the positive pressure on face A, making it less prominent. Meanwhile, faces CEF and G face more substantial negative pressure coefficients due to their alignment with the wind direction

At this 60-degree angle, face G, positioned diametrically opposite to face B, experiences a substantial negative pressure compared to faces CEF. Consequently, there is a noteworthy likelihood of suction formation on face G, resulting in a negative pressure magnitude greater than the direct positive pressure experienced by the prominent faces B and C.

At this 90-degree angle, face B, being a curved surface adjacent to face C, undergoes a lesser negative pressure compared to faces AEF. Apart from surface B, all other faces of the building share the same negative pressure coefficients.

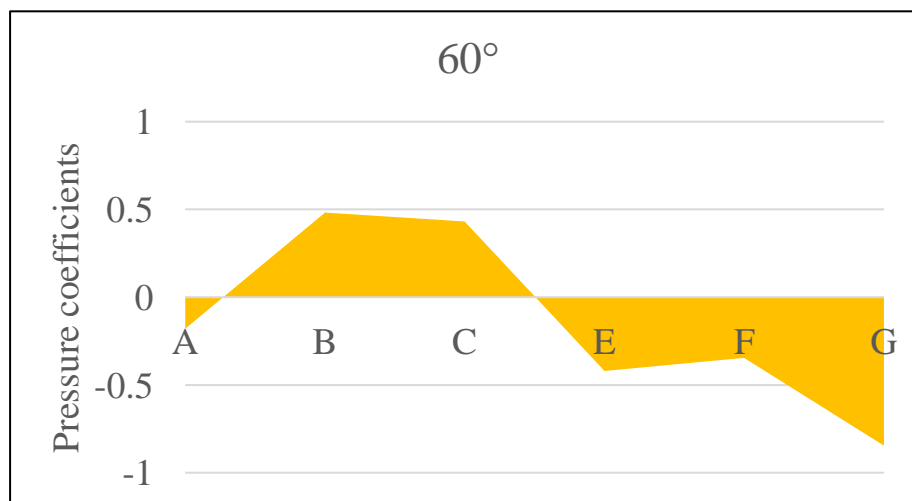


Figure 11: variation in pressure coefficients at 60°



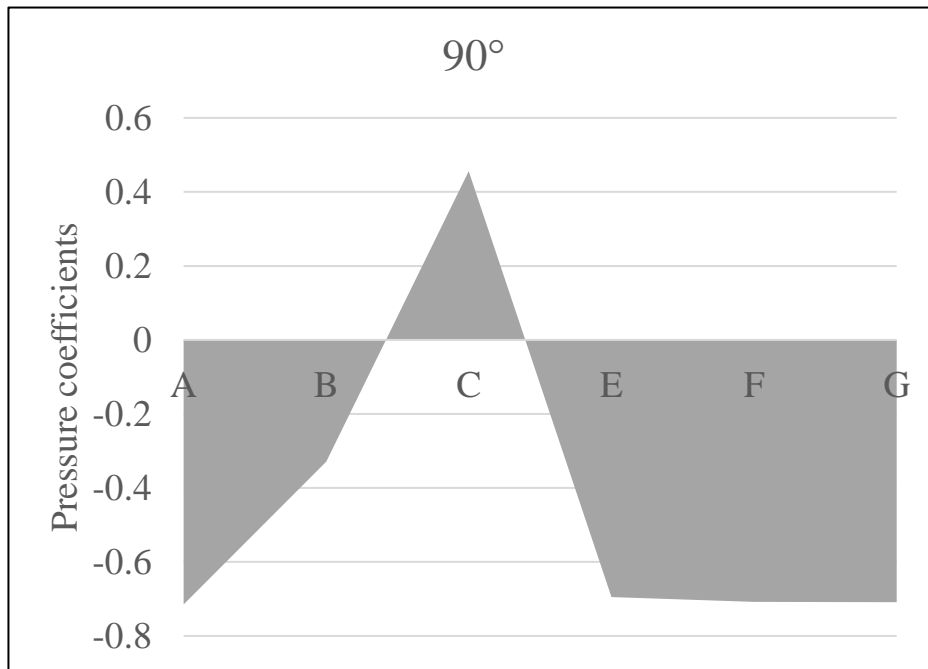


Figure 12: variation in pressure coefficients at 90°

Under a wind load acting at a 180-degree angle to the featured building, the primary surfaces, namely face E, face F, and face G, experience positive pressure coefficients. In contrast, other surfaces like AB and C undergo negative

pressure coefficients. This means that faces E, F, and G are subjected to increased air pressure, while faces AB and C face reduced air pressure. The distribution of pressure coefficients provides insights into how the wind interacts with different parts of the building, influencing factors such as structural stability and aerodynamic performance.

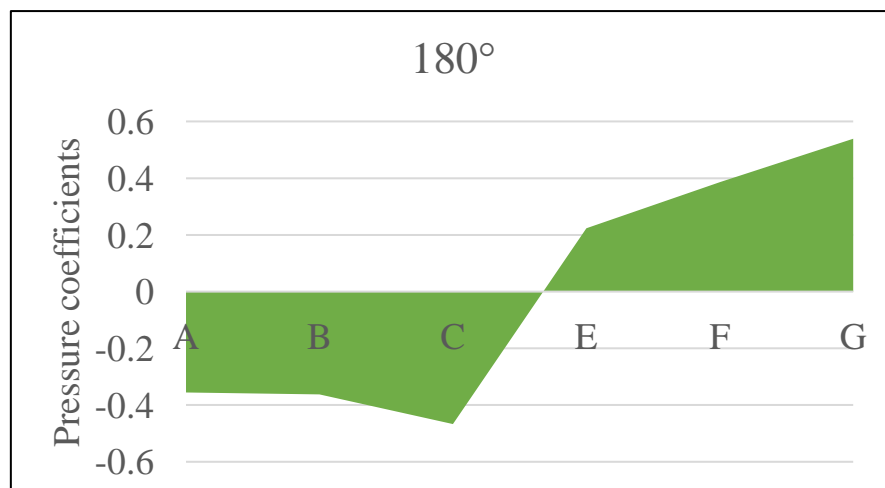


Figure 13: variation in pressure coefficients at 180°

#### 4 Conclusions

The current investigation demonstrates that the model shape, arrangement, and angle of incidence have a substantial impact on the pressure exerted on the model building. The important findings of this investigation are summed up as follows:

1. The main objective of this investigation is mean pressure coefficients. The front face of A has the highest positive mean pressure coefficients, whereas the inner face G of the model has the most negative pressure coefficients.
2. It is proved that the structure's variation in pressure is directly impacted by the wind flow pattern.
3. We also got to know that the dynamic behavior of wind flow that causes vortex creation are various mechanisms including flow separation, up wash, and downwash.

---

**5 REFERENCE:**

- [1] Bhattacharyya B, Dalui SK, Ahuja AK (2014) Wind-induced pressure on ‘E’ plan shaped tall buildings. *Jordan J Civil Eng* 8(2):120–13.
- [2] Raj R, Ahuja AK (2013) Wind loads on cross shape tall buildings. *J Acad Ind Res (JAIR)* 2(2):111
- [3] Li, Y., Li, Q. S., & Chen, F. (2017). Wind tunnel study of wind-induced torques on L-shaped tall buildings. *Journal of Wind Engineering and Industrial Aerodynamics*, 167, 41-50.
- [4] Mukherjee, S., Chakraborty, S., Dalui, S.K. and Ahuja, A.K. (2016), “Wind Induced pressure on Z plan shape tall building”, *Wind Struct.*, 19(5), 523-540.
- [5] Kar, R., & Dalui, S. K. (2022). Wind-interference effect on an octagonal building in varying positions by large eddy simulation. *Advances in Structural Engineering*, 25(1), 201-211.
- [6] Kar, R.; Dalui, S.K.: Wind interference effect on an octagonal plan shaped tall building due to square plan shaped tall buildings. *Int. J. Adv. Struct. Eng.* 8, 73–86 (2016). <https://doi.org/10.1007/s40091-016-0115-z>
- [7] Liang S, Li QS, Lui S, Zhang L, Gu M (2004) Torsional dynamic wind loads on rectangular tall buildings. *Eng Struct* 26(2004):129–137
- [8] Sanyal, P., & Dalui, S. K. (2021, August). Effects of side ratio for ‘Y’ plan shaped tall building under wind load. In *Building Simulation* (Vol. 14, No. 4, pp. 1221-1236). Tsinghua University Press.
- [9] Pal, S., & Raj, R. (2021). Evaluation of wind-induced interference effects on shape remodeled tall buildings. *Arabian Journal for Science and Engineering*, 46(11), 11425-11445.
- [10] Kheyari P, Dalui SK (2015) Estimation of wind load on a tall building under interference effects: a case study. *Jordan J Civil Eng* 9(1):84–101
- [11] Singh, J., & Roy, A. K. (2019). Effects of roof slope and wind direction on wind pressure distribution on the roof of a square plan pyramidal low-rise building using CFD simulation. *International Journal of Advanced Structural Engineering*, 11(2), 231-254.
- [12] Sanyal, P., & Dalui, S. K. (2018). Effects of courtyard and opening on a rectangular plan-shaped tall building under wind load. *International Journal of Advanced Structural Engineering*, 10(2), 169-188.
- [13] Chand I, Bhargava PK (1992) Studies on the effect of mean wind speed profile on the height of air layer affected by buildings. *Renew Energy* 2:507–512
- [14] Chand I, Sharma VK, Bhargava PK (1995) Effect of Neighbouring Buildings on Mean Wind Pressure Distribution on a Flat Roof. *Archit Sci Rev* 38:29–36. <https://doi.org/10.1080/00038628.1995.9696773>
- [15] Kareem A (1986) The effect of Aerodynamic interference on the dynamic response of prismatic structures. *J Wind Eng Ind Aerodyn* 25(1987):365–372
- [16] Yi, J., & Li, Q. S. (2015). Wind tunnel and full-scale study of wind effects on a super-tall building. *Journal of Fluids and Structures*, 58, 236-253.
- [17] Bhattacharyya, B., & Dalui, S. K. (2020). Experimental and numerical study of wind-pressure distribution on irregular-plan-shaped buildings. *Journal of Structural Engineering*, 146(7), 04020137
- [18] Xing, F., Mohotti, D., & Chauhan, K. (2018). Experimental and numerical study on mean pressure distributions around an isolated gable roof building with and without openings. *Building and Environment*, 132, 30-44
- [19] IS 875 (Part 3)-1987 Indian Standard code of practice for design loads (other than earthquake) for building and structures, bureau of Indian standard, New Delhi

- [20] Franke, J., Hirsch, C., Jensen, A. G., Krüs, H. W., Schatzmann, M., Westbury, P. S., ... & Wright, N. G. (2004, May). Recommendations on the use of CFD in predicting pedestrian wind environment. In *Cost action C* (Vol. 14).
- [21] Lam, K.M., Wong, S.Y. and To, A.P. (2009), "Dynamic wind loading of H-shaped tall buildings", Proceedings of the 7th Asia-Pacific Conference on Wind Engineering, Taipei, Japan, November.
- [22] Wang, Q., Zhang, G., Li, W., & Shi, L. (2020). Numerical simulation of two-way fluid-structure interaction of wind loading on buildings. *Journal of the Chinese Institute of Engineers*, 43(3), 225-240.
- [23] Mohotti, D., Mendis, P., & Ngo, T. (2013). Application of Computational Fluid Dynamics (CFD) in Wind Analysis of Tall Buildings. *no. December*.
- [24] Mallick, M., Mohanta, A., Kumar, A., & Raj, V. (2018). Modelling of wind pressure coefficients on C-shaped building models. *Modelling and Simulation in Engineering, 2018*.
- [25] Feng, C., Gu, M., & Zheng, D. (2019). Numerical simulation of wind effects on super high-rise buildings considering wind veering with height based on CFD. *Journal of Fluids and Structures*, 91, 102715.
- [26] Parv, B., Hulea, R., & Mircea, Z. R. (2012). Comparative study of wind effects on tall buildings using international codes and CFD. In *European Congress on Computational Methods in Applied Sciences and Engineering (ECCOMAS)*.
- [27] Kummitha, O. R., Kumar, R. V., & Krishna, V. M. (2021). CFD analysis for airflow distribution of a conventional building plan for different wind directions. *Journal of Computational Design and Engineering*, 8(2), 559-569.
- [28] Lee, D. S. H. (2017). Impacts of surrounding building layers in CFD wind simulations. *Energy Procedia*, 122, 50-55.
- [29] Mukherjee, A., & Bairagi, A. K. (2017). Wind pressure and velocity pattern around 'N'plan shape tall building—A case study. *Asian J. Civil Eng. (BHRC)*, 18(8), 1241-1258.
- [30] Assainar, N., & Dalui, S. K. (2021). Aerodynamic analysis of pentagon-shaped tall buildings. *Asian Journal of Civil Engineering*, 22(1), 33-48.
- [31] Deng, T., Fu, J. Y., Xie, Z. N., Pi, Y. L., & Shi, B. Q. (2018). An experimental study on the wind pressure distribution of tapered super high-rise buildings. *The Structural Design of Tall and Special Buildings*, 27(13), e1483.